Annals of Oral & Maxillofacial Surgery
Open Access

Emerging Technologies

Research study

Composite polymer-coated mineral grafts for bone regeneration: material characterisation and model study

G Pertici[1,2], F Rossi[3], T Casalini[3], G Perale[1,2,4]*

Abstract

Introduction

This study discusses composite polymer-coated mineral grafts for bone regeneration.

Materials and Methods

Bone xenografts are coated with degradable synthetic [poly(L-lactide-co-ε-caprolactone)] and natural (polysaccharides) polymers in order to increase their mechanical properties, on one side, and to improve cell adhesion, on the other, with the purpose of developing a novel composite material for bone tissue engineering. *In vitro* assays help examine the microstructure of the scaffold by Fourier transform infrared and environmental scanning electron microscopy analyses and the porosity of the material by micro-computed tomography. The good adhesion property of polymer coated on to the mineral scaffold is deeply analysed and proved. The *in vitro* polymer degradation, in terms of time evolution of polymer-coating thickness, was rationalised with a mathematical model. The purpose of such modelling activity is to provide a simple but powerful tool to understand the influence of design parameters on coating behaviour.

Results

The fabricated bone graft exhibited regular microstructure similar to healthy iliac bones with an average of 27% open porosity and an adequately rigid structure, which ensures a better osteointegration once implanted.

Conclusion

This approach avoids the use of trial-and-error methods and consents a better *a priori* material design.

* Corresponding author
Email: giuseppe@ibi-sa.com

[1] Industrie Biomediche Insubri S.A, Mezzovico-Vira, Switzerland
[2] Department of Innovative Technologies, University for Applied Science and Art of Southern Switzerland, Switzerland
[3] Department of Chemistry, Materials and Chemical Engineering "Giulio Natta", Politecnico di Milano, Milan, Italy
[4] Swiss Institute for Regenerative Medicine, Taverne, Switzerland

Introduction

A critical-sized defect is a large disruption in a bony tissue, either a fracture or a hole that cannot spontaneously heal, and the actual size varies depending on the species and anatomical site[1–3]. In this framework, particularly, the restoration of mandibular defects caused by ablative surgery for oral and maxillofacial tumour, trauma, infection and congenital deformity remains a challenge for surgeons[4,5]. Hence, the need of adequate bone substitutes for remodelling of native bone tissue is evident and requires a wide spectrum of proposed solutions, belonging to academia, clinics and industry[6–8]. Nowadays, autologous grafting and distraction osteogenesis are most common techniques used to restore mandibular defects[9,10]. Generally, autologous grafts have been considered the 'gold standard' because of the advantages of osteogenesis, osteoinduction and osteoconduction[11]. However, major drawbacks of these methods are severe morbidity, as well as donor-site availability, which call for new methods and solutions for bone reconstruction[12–15]. Naturally derived materials, most commonly of animal origin (xenografts), provide structures similar to living tissues that might induce specific cellular responses and sometimes also supersede the advantages of synthetic polymers, which indeed represent another viable alternative to autografts[16–18]. Xenografts may also reduce the stimulation of chronic inflammation or immunological reactions and toxicity, which, on the other hand, are often detected with synthetic polymers[16,19,20]. Nowadays, materials science, in conjunction with bio- and nanotechnologies, provides interesting solutions for the design of better performing bone[7,21–24]. In particular, biodegradable scaffolds are widely used as key artificial medical devices in tissue engineering, which aim to provide a desirable microenvironment that allows neo-tissue to be generated to repair and replace damaged or missing bone districts[25–27]. Indeed, innovative synthetic polymers can be tuned in terms of composition, rate of degradation, mechanical and chemical properties[16,19]. As a fundamental premise in tissue engineering, polymeric scaffold should provide (a) host tissue-like mechanical support for promoting neo-tissue growth and functioning[28]; (b) adequate porosity and permeability for nutrient delivery and metabolite removal[29] and (c) a controllable degradation rate of the matrix[30]. But, even further progresses in tissue engineering, combining natural and synthetic components, could yield more favourable outcomes than current range of approaches used to repair, e.g. maxillo-cranial, facial, palate and calvarial defects[2,9,31]. Hence, the goal of the proposed approach was to combine the biocompatibility and tissue integration capability of natural materials with the possibility to tune mechanical and physical

Licensee OA Publishing London 2014. Creative Commons Attribution License (CC-BY)

FOR CITATION PURPOSES: *Pertici G, Rossi F, Casalini T, Perale G.* Composite polymer-coated mineral grafts for bone regeneration: material characterisation and model study. Annals of Oral & Maxillofacial Surgery 2014 Feb 14;2(1):4.

Competing interests: none declared. Conflict of interests: none declared.
All authors contributed to conception and design, manuscript preparation, read and approved the final manuscript.
All authors abide by the Association for Medical Ethics (AME) ethical rules of disclosure.

Annals of Oral & Maxillofacial Surgery
Open Access

Research study

properties, typical of synthetic ones. Our bone graft, known as SmartBone® (SB), is hence a composite material that was obtained using bovine bone-derived matrix as starting material, reinforced with poly(L-lactide-co-ε-caprolactone) (PLCL) and polysaccharides. The bovine-derived matrix[32] is a mineral matrix made of calcium hydroxyapatite [HA, $Ca_5(PO_4)_3(OH)$] and very minor collagen residuals that present a chemical microstructure and a micromorphology that resembles the human bone[33–35]. However, as said above, its physical properties evidence a rigid, but not elastic, structure and thus too fragile for any reconstructive surgery applications. In addition, the due cleaning and sterilisation processes destroy its biochemical structure, increase structural porosity and hence allow neither easy graft handling nor cell adhesion. It is in this framework that our approach finds its core aims to reinforce a bovine-derived bone structure with the addition of an elastic component in terms of polymer coating, thus loosing fragility and reducing porosity, and to resemble healthy human bone[36]. Finally, the addition of polysaccharides, even in extremely low quantities, increases the hydrophilicity of the scaffold with consequent higher blood affinity and favouring cell attachment, thus enhancing biocompatibility and osteointegration[6,36]. The grafts were characterised in terms of chemical composition, microstructure, physical properties and polymer-coating degradation. The resulting composite material has been proved to be able to mimic human bone microstructure and to ensure macro-scale properties, which include an adequate-sized open porosity with combined rigid–elastic behaviour, together with surface properties ensuring cell viability and fast tissue integration.

In addition, the proper design of coating was performed using a mathematical model that can help material design avoid classic 'trial-and-error' approaches[37,38]. The aim of this study was to perform a model study and characterise the materials used in composite polymer-coated mineral grafts for bone regeneration.

Materials and Methods

Materials and scaffold preparation

The bovine-derived cancellous bone was sourced as described in a study conducted by Pertici et al.[39], being certified for human uses. The choice of polymers was based on their potential applicability within the pharmaceutical and biomedical industries and the necessity to obtain scaffolds with suitable mechanical properties. A commercially available copolymer of poly(L-lactic acid) and poly(ε-caprolactone), already used in medical applications, was chosen (Purac Biomaterials, Gorinchem, The Netherlands). Polysaccharides (Merck, Darmstadt, Germany) were also chosen in order to improve the hydrophilicity of the matrix. All materials were used as received. SB grafts were then obtained by reinforcing bovine bone-derived matrix with the mixture of PLCL and polysaccharides through a proprietary process[39,40]. Ethylene oxide sterilisation (at BioSter SpA, Bergamo, Italy) was applied after final double layer packing.

Fourier transform infrared spectroscopy

Samples were laminated with potassium bromide and then recorded using Thermo Nexus 6700 spectrometer coupled to Thermo Nicolet Continuum microscope equipped with a 15× Reflachromat Cassegrain objective.

Environmental scanning electron microscopy analysis

Environmental scanning electron microscopy (ESEM) analysis and energy-dispersive analysis (EDS) were performed at 10 kV with Evo 50 EP Instrumentation (Zeiss, Jena, Germany). Each sample was first analysed on the side surfaces and then halved with a sharp scalpel and the two inner exposed surfaces were finally analysed.

Micro-computed tomography imaging

Five cubic samples of SB were cut to about 8 mm in side length, for the sake of instrumental cell dimension, mounted and scanned with micro-computed tomography (micro-CT) system (VTomEx-s, Phoenix|x-ray, a GE Healthcare Company, Little Chalfont, Buckinghamshire, UK. The images consisted of 936 slices with a voxel size of 21 μm in all three axes. The scaffolds were imaged and reconstructed in three dimensions. Regions of interest (ROI) adjacent to implants of the same size were reconstructed and analysed using micro-CT with the same thresholds. The database was analysed and three-dimensional pictures of each ROI were obtained. From acquired data, graft free volume (ε) and surface/volume ratio were estimated.

Degradation studies: model development

For the sake of simplicity, the system is represented as a cubic lattice containing spherical pores. The number and the size of the pores can be consistently determined starting from the surface area and the void ratio determined with micro-CT analysis:

$$N_p \cdot \frac{4}{3} \cdot \pi \cdot r^3 = \varepsilon \cdot V \quad (1)$$

$$N_p \cdot 4 \cdot \pi \cdot r^2 = S \quad (2)$$

Where N_p is the pore number, r is the pore radius, ε is the void ratio, V is the device volume and S is the surface area. Polymer coating is assumed to be homogeneous and uniformly distributed as spherical shells inside the pores; coating thickness can be computed as follows:

$$\frac{V_{\text{pol}}}{N_p} = \frac{4}{3} \cdot \pi \cdot \left[r^3 - (r - r_{\text{pol}})^3 \right] \quad (3)$$

Where V_{pol} is the total polymer volume in the system and r_{pol} is the

Licensee OA Publishing London 2014. Creative Commons Attribution License (CC-BY)

FOR CITATION PURPOSES: *Pertici G, Rossi F, Casalini T, Perale G.* Composite polymer-coated mineral grafts for bone regeneration: material characterisation and model study. Annals of Oral & Maxillofacial Surgery 2014 Feb 14;2(1):4.

Competing interests: none declared. Conflict of interests: none declared.
All authors contributed to conception and design, manuscript preparation, read and approved the final manuscript.
All authors abide by the Association for Medical Ethics (AME) ethical rules of disclosure.

Annals of Oral & Maxillofacial Surgery
Open Access

Research study

spherical coating thickness. Polymer degradation occurs according to hydrolysis mechanism, where water breaks long chains in small oligomers:

$$P_{n+m} + W \leftrightarrow P_n + P_m \quad (4)$$

where W is water and P_n is a generic polymer chain with n monomer units.

System dynamics is described through mass conservation equations, applying the method of the moments. This approach, already proposed by Perale et al.[38], was chosen for its validated results[41–44]. Polymer degradation is then represented with following system of partial differential equations:

$$\frac{\partial C_M}{\partial t} = \nabla(D_M \nabla C_M) - 2k_P C_M \mu_0 + \frac{k_P}{K_{EQ}} C_W (\mu_0 - C_M) \quad (5a)$$

$$\frac{\partial C_W}{\partial t} = \nabla\left(D_W \nabla C_W\right) + k_P \mu_0^2 - \frac{k_P}{K_{EQ}} C_W (\mu_1 - \mu_0) \quad (5b)$$

$$\frac{\partial \mu_0}{\partial t} = \nabla(D_M \nabla C_M) - k_P \mu_0^2 + \frac{k_P}{K_{EQ}} C_W (\mu_1 - \mu_0) \quad (5c)$$

$$\frac{\partial \mu_1}{\partial t} = \nabla(D_M \nabla C_M) \quad (5d)$$

$$\frac{\partial \mu_2}{\partial t} = \nabla(D_M \nabla C_M) + 2k_P \mu_1^2 + \frac{k_P C_W}{3K_{EQ}} \left(\mu_1 - 2\frac{\mu_2^2}{\mu_1} + \frac{\mu_2 \mu_1}{\mu_0}\right) \quad (5e)$$

$$\frac{\partial s}{\partial t} = -k_c \cdot C_{M,\text{int}} \cdot MW_{\text{mon}} \cdot \frac{1}{\rho_{\text{pol}}} \quad (5f)$$

Equation details have been widely explained elsewhere[38,41]. Diffusion coefficients are effective values, as they are related to the degradation process through a functional dependence on average numeral molecular weight[41,44]:

$$D = \frac{12}{25} D_i^0 \exp\left(2.5\left(1 - \frac{MW_n(t,r)}{MW_n(t=0)}\right)^{0.5}\right)$$

i = monomer, water (6)

$$MW_n = \frac{\mu_1}{\mu_0} MW_{\text{mon}} \quad (7)$$

Derivative terms are expressed in spherical coordinates, taking into account only radial terms, in which radius is the characteristic degradation length. Equation (5f) describes the coating thickness reduction because of mass transfer between the polymer phase and the surrounding environment. Such formalism is allowed because, for such system, the mass transfer (*i.e.* polymer dissolution from the coating surface to the surrounding environment) plays a key role in the overall behaviour, as illustrated by means of a characteristic times analysis (*vide infra*).

Estimation of parameters

Average weight, number, molecular weight as well as the polydispersity are estimated from producer data, while monomer molecular weight and polymer density are weighted average values with respect to polymer composition. Polymerisation kinetic constant was estimated as explained in Lemmouchi et al.[42] who studied degradation behaviour of various aliphatic polyesters formulations. In particular, model was adapted in order to reproduce experimental data of molecular weight, which indicates decrease in cylindrical devices of PLCL 80:20. Monomer and water diffusivity represent a reasonable estimation for aliphatic polyester formulations[33] (Table 1).

Results

Chemical structure

Macroscopic view of a 10×10×10 mm SB graft is presented in Figure 1(a), which is a macroscopic view that confirms its porous structure with small and interconnected pores. Its chemical structure was studied using Fourier transform infrared (FT-IR) analysis, as presented in Figure 1(b). The peak corresponding to 3450 cm^{-1} belongs to –OH groups, and 2960 cm^{-1} represents stretching vibration of CH_3. The presence of PLCL polymer coating is evidenced not only by peak at 2960 cm^{-1} (CH_3), but also by peaks at 1460 and 1100 cm^{-1}, carbonyl (1640 cm^{-1}) and C–O–C groups, respectively. The presence of polysaccharide is visible from C–O–C groups, overlapped with polymer signal. The mineral nature of the matrix is underlined by the presence of phosphate groups typical of HA and revealed by 1050 and 600 cm^{-1} peaks[45].

Table 1 Simulation input data

Monomer molecular weight	MW_{mon} = 97.3 mg/mmol
Polymer Density	ρ = 1200 mg/cm³
Average number molecular weight	MW_n = 136000 mg/mmol
Average weight molecular weight	MW_w = 204000 mg/mmol
Monomer effecitve diffusvity	D_M = 3.6 10^{-5} mm²/h
Water effective diffusvity	D_w = 3.6 10^{-3} mm²/h
Polymerisation kinetic constant	k_p = 6.7135 .10^{-7} mm³/mmol/h
Equilibrium constant	KE_Q = 10^{-3}
Polydispersity	P_D = 1.5

Licensee OA Publishing London 2014. Creative Commons Attribution License (CC-BY)

FOR CITATION PURPOSES: *Pertici G, Rossi F, Casalini T, Perale G.* Composite polymer-coated mineral grafts for bone regeneration: material characterisation and model study. Annals of Oral & Maxillofacial Surgery 2014 Feb 14;2(1):4.

Competing interests: none declared. Conflict of interests: none declared.
All authors contributed to conception and design, manuscript preparation, read and approved the final manuscript.
All authors abide by the Association for Medical Ethics (AME) ethical rules of disclosure.

Annals of Oral & Maxillofacial Surgery
Open Access

Research study

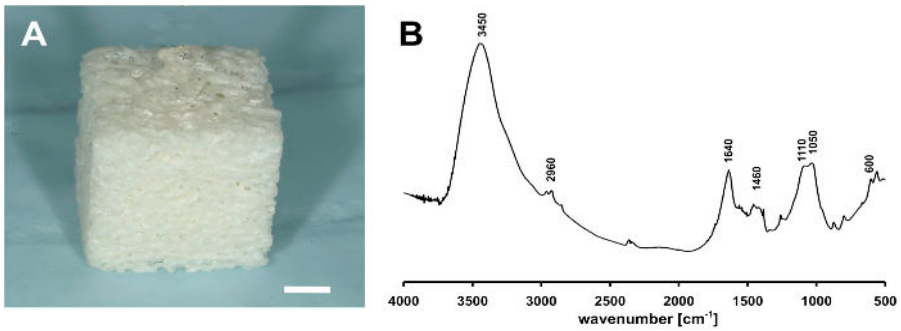

Figure 1: (a) Macroscopic view of SB graft (scale bar = 2.5 mm) and (b) FT-IR spectra of a cross-section of the SB graft. FT-IR, Fourier transform infrared; SB, SmartBone®.

Studying pore structure with micro-computed tomography and environmental scanning electron microscopic analyses

SB grafts were scanned to study its porosity at high resolution using a micro-CT scanner. 2D and 3D reconstruction confirms interconnected open porous structure through the whole thickness of the scaffold (Figure 2(a) and (b)). Average tested scaffolds resulted in an equivalent volume of about 515 mm^3, a free volume of 140 mm^3 and a surface of 2,300 mm^2. Moreover, the average porosity of samples (ε) was found to be 0.27 and the ratio between surface and volume was 4.46 mm^{-1}. All measures showed <15% standard deviation values.

Native bovine-derived bone matrix was analysed from a microstructural point of view using ESEM and its structure is shown in Figure 3(a).

Polymer degradation

Coating degradation has been modelled through the system of partial differential equations constituted by eqs. 5a-f. The numerical integration, performed by means of ode15s algorithm as implemented in MATLAB, allowed obtaining the time evolution of coating thickness (Figure 4d) for four different initial thickness values. The robustness and the consistency of the adopted approach have been evaluated through a characteristic times analysis.

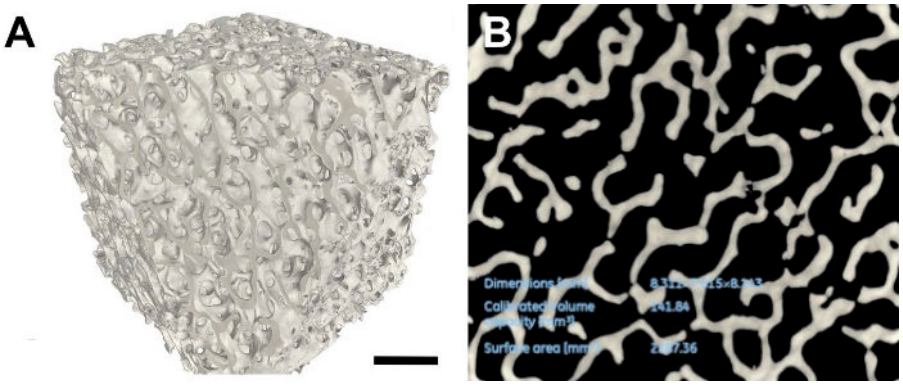

Figure 2: (a) 3D reconstruction of porous structure by micro-CT scanning and (b) representative image of one slice of 2D micro-CT scanning (scale bar = 2.5 mm). 2D, two dimensional; 3D, three dimensional; micro-CT, micro-computed tomography.

Discussion

Scaffolds morphology

As mentioned, a microstructural analysis of native bovine-derived bone matrix was carried out using ESEM, as shown in Figure 3(a). Pores are well distributed along the sample, but they are extremely larger with respect to the ones present in healthy human iliac crest bones. As is well-known[46], porosity and pore size of biomaterials play a key role in osteointegration and new bone formation; indeed, relatively larger pores favour direct osteogenesis, as they allow vascularisation and high oxygenation, while smaller ones result in osteochondral ossification. There is, however, an upper limit for porosity and pore size set by constraints associated with mechanical properties. An increase in the empty volume results in a reduction in mechanical strength of the graft, which can be critical for regeneration of load-bearing sites. Differences in bone tissues in morphological (pore size and porosity) and mechanical properties have set challenges for fabricating biomaterial scaffolds that can meet the requirements set by the specific site of application. So, following these statements, polymer reinforcement, present in SB sample, seems to be essential to reduce the pore sizes presented in Figure 3(b). The analysis of the inner surface of the sample (Figure 3c) reveals that the porous mineral structure and polymer are easily distinguishable. Owing to their properties, mineral part appears as brighter, as in Figure 3(c), while polymer coating appears darker. EDS of zone 1 is characterised by strong signals of C and O, confirming the presence of the polymeric film; while spectrum 2, by the presence of Ca and P, shows the mineral part of the sample corresponding to HA (Figure 3d).

Mathematical modelling of polymer degradation

As recently reviewed[47], mathematical modelling is extremely powerful

Licensee OA Publishing London 2014. Creative Commons Attribution License (CC-BY)

FOR CITATION PURPOSES: *Pertici G, Rossi F, Casalini T, Perale G.* Composite polymer-coated mineral grafts for bone regeneration: material characterisation and model study. Annals of Oral & Maxillofacial Surgery 2014 Feb 14;2(1):4.

Competing interests: none declared. Conflict of interests: none declared.
All authors contributed to conception and design, manuscript preparation, read and approved the final manuscript.
All authors abide by the Association for Medical Ethics (AME) ethical rules of disclosure.

Annals of Oral & Maxillofacial Surgery
Open Access

Research study

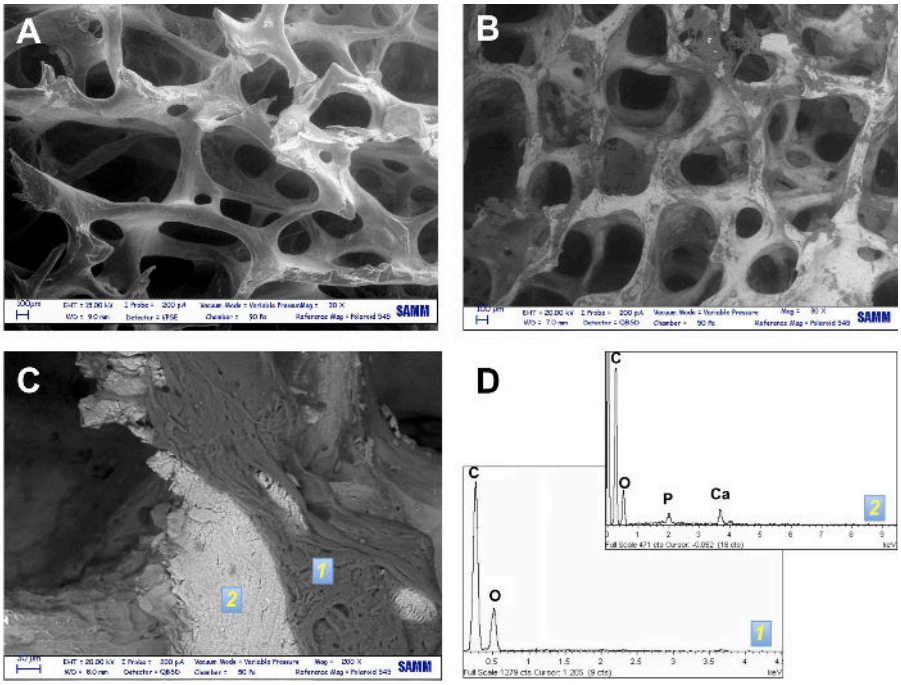

Figure 3: ESEM images at the same magnitude (bar scales = 100 μm) of bovine bone matrix (a) and polymer-coated SB graft (b). (c, d) ESEM image of SB graft (scale bar = 30 μm) and corresponding EDS spectra. Spot 2 is characterised only by strong signals of C and O, typical of the presence of polymer film; and spot 1 is characterised by the presence of Ca and P, confirming the mineral nature of the matrix. EDS, energy-dispersive analysis; ESEM, environmental scanning electron microscopy; SB, SmartBone®.

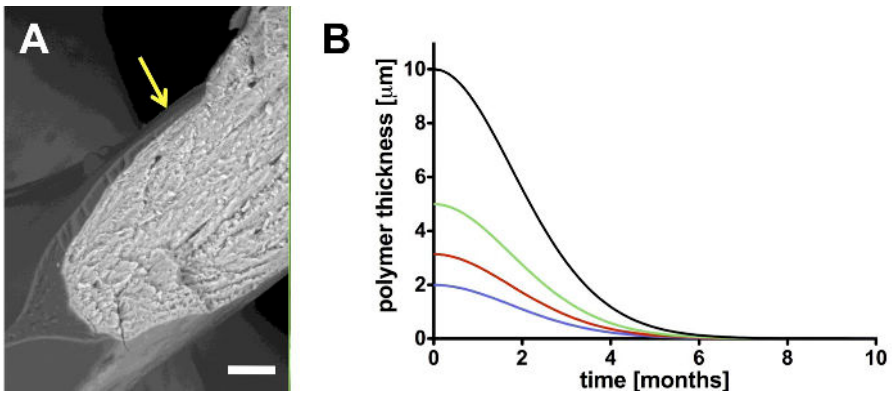

Figure 4: (a) ESEM image of polymer coated on to mineral matrix (yellow arrow, scale bar = 20 μm) and (b) polymeric PLCL coating degradation from SB grafts with different coating thicknesses (blue = 2 μm, red = 3 μm, green = 5 μm, black = 10 μm). ESEM, environmental scanning electron microscopy; PLCL, poly(L-lactide-co-ε-caprolactone); SB, SmartBone®.

in describing the polymer degradation behaviour[37,38,41], particularly when assuming that *in vivo* degradation follows the same kinetics of the *in vitro* degradation. This is undoubtedly a key aspect that is currently widely investigated in the literature, where nevertheless the mostly accepted approach suggests that *in vivo* degradation of thin polymeric film is faster by at least a factor of 2 with respect to *in vitro* simulations[38,48].

The consistency and robustness of the adopted approach can be verified, as mentioned, through a characteristic time analysis. The diffusion characteristic time can be computed as follows:

$$\tau_D = \frac{s^2}{D_M^0} \approx 0.027 - 2.7h \qquad (8)$$

where s is coating thickness (which ranges from 1 to 10 μm, in this calculation) and D_M^0 is monomer diffusion coefficient. Diffusion characteristic time is fast, and this could be because of the low coating thickness; indeed, calculation showed that, at each time step, monomer concentration profiles are practically uniform along the coating.

Degradation time can be defined as follows:

$$\tau_{depol} = \frac{K_{EQ}}{k_p C_W} \approx 9000\text{h} \qquad (9)$$

where K_{EQ} is the equilibrium constant, k_p is the polymerisation constant and C_W is water concentration. De-polymerisation constant (*i.e.* the ratio between k_p and K_{EQ}) is tripled in order to reproduce *in vivo* degradation[38,48]. The mass transfer characteristic time can be written as:

$$\tau_{mt} = \frac{1}{k_C a} \approx 0.86 - 8.6\,\text{h} \qquad (10)$$

where k_C is mass transfer coefficient (computed from Sherwood number, equal to 2 for such systems[49], and computed for coating thickness values ranging from 1 to 10 μm) and a is the specific mass transfer surface. It can be observed that τ_{mt} is about 2 orders of magnitude lower than τ_{depol}, suggesting that monomer dissolution from the surface is promoted over depolymerisation. Moreover, diffusion characteristic time is lower than mass transfer, which highlights that transport phenomena inside the coating do not play a relevant role in the overall system behaviour.

Licensee OA Publishing London 2014. Creative Commons Attribution License (CC-BY)

FOR CITATION PURPOSES: *Pertici G, Rossi F, Casalini T, Perale G.* Composite polymer-coated mineral grafts for bone regeneration: material characterisation and model study. Annals of Oral & Maxillofacial Surgery 2014 Feb 14;2(1):4.

Competing interests: none declared. Conflict of interests: none declared.
All authors contributed to conception and design, manuscript preparation, read and approved the final manuscript.
All authors abide by the Association for Medical Ethics (AME) ethical rules of disclosure.

Annals of Oral & Maxillofacial Surgery
Open Access

Coating thickness is clearly visible in Figure 4(a), obtained again thanks to a very precise and sharp cut that evidences the polymer coated on to the mineral matrix. Hence, as mentioned, depolymerisation kinetics is tripled in order to best adhere to the reality. The practical need, here, was to obtain a reliable description of thickness reduction in time once *in vivo*, which easily allowed to compute, as shown in Figure 4(b). In the first 2 months, the degradation occurs with the thinning of the film, as expected; from the end of the third month, the degradation reaches such a point from where a dramatic film thinning starts, leading to complete film dissolution between the fourth and the sixth months. Plots presented in Figure 4(b) show the behaviour of different thicknesses that can be present at day 0 (2, 3, 5 and 10 μm). Indeed, as seen before, the film coverage is statistically regular but some dishomogeneities might be present, mainly because of the natural origin of the mineral substrate. Nevertheless, the film being always much below critical thickness, the surface erosion process allows degradation, which follows the same pattern and lets the film degrade within 4–5 months, *de facto* independently form starting thickness.

Conclusion

In this study, a composite graft made of natural mineral matrix (calcium HA) and synthetic polymer coating (PLCL) with the addition of polysaccharides was developed. The purpose behind coating mineral matrix with PLCL and polysaccharides comes from the necessity to have higher mechanical properties together with suitable microstructure, on one side, and to improve hydrophilicity for good cell adhesion, on the other. The fabricated bone graft exhibited regular microstructure similar to healthy iliac bones with an average 27% porosity. The chemical structure of the graft was verified with FT-IR and EDS, underlining the good adhesion between polymer coating and HA. PLCL coating degradation was studied and related to its thickness using a well-known mathematical model. This approach avoids the use of trial-and-error methods and consents a better *a priori* material design.

Abbreviations list

EDS, energy-dispersive analysis; ESEM, Environmental scanning electron microscopy; FT-IR, Fourier transform infrared; HA, hydroxyapatite; micro-CT, micro-computed tomography; PLCL, poly(L-lactide-co-ε-caprolactone); ROI, regions of interest; SB, SmartBone®.

Acknowledgement

The authors thank Phoenix|x-ray (a GE company) for the support with the micro-CT analysis.

References

1. Cordonnier T, Sohier J, Rosset P, Layrolle P. Biomimetic materials for bone tissue engineering–state of the art and future trends. Adv Eng Mat. 2011 May;13(5):B135–50.
2. Chen FM, An Y, Zhang R, Zhang M. New insights into and novel applications of release technology for periodontal reconstructive therapies. J Control Release. 2011 Jan;149(2):92–110.
3. Mourino V, Boccaccini AR. Bone tissue engineering therapeutics: controlled drug delivery in three-dimensional scaffolds. J R Soc Interface. 2010 Feb;7(43):209–27.
4. Zhou M, Peng X, Mao C, Xu F, Hu M, Yu G. Primate mandibular reconstruction with prefabricated, vascularized tissue-engineered bone flaps and recombinant human bone morphogenetic protein-2 implanted in situ. Biomaterials. 2010 Jun;31(18):4935–43.
5. Gronthos S. Reconstruction of human mandible by tissue engineering. Lancet. 2004 Aug;364(9436):735–6.
6. Isikli C, Hasirci V, Hasirci N. Development of porous chitosan–gelatin/hydroxyapatite composite scaffolds for hard tissue-engineering applications. J Tissue Eng Regen Med. 2012 Feb;6(3):135–43.
7. Langer R. Perspectives and challenges in tissue engineering and regenerative medicine. Adv Mater. 2009 Sep;21(32–33):3235–6.
8. Hutmacher DW, Schantz JT, Lam CX, Tan KC, Lim TC. State of the art and future directions of scaffold-based bone engineering from a biomaterials perspective. J Tissue Eng Regen Med. 2007 Jul–Aug;1(4):245–60.
9. Zou D, Zhang Z, He J, Zhu S, Wang S, Zhang W, et al. Repairing critical-sized calvarial defects with BMSCs modified by a constitutively active form of hypoxia-inducible factor-1α and a phosphate cement scaffold. Biomaterials. 2011 Dec;32(36):9707–18.
10. Di Stefano DA, Artese L, Iezzi G, Piattelli A, Pagnutti S, Piccirilli M, Perrotti V. Alveolar ridge regeneration with equine spongy bone: a clinical, histological, and immunohistochemical case series. Clin Implant Dent Relat Res. 2009 Jun;11(2):90–100.
11. Samavedi S, Whittington AR, Goldstein AS. Calcium phosphate ceramics in bone tissue engineering: a review of properties and their influence on cell behavior. Acta Biomater. 2013 Sep;9(9):8037–45.
12. Chen M, Le DQ, Baatrup A, Nygaard JV, Hein S, Bjerre L, et al. Self-assembled composite matrix in a hierarchical 3-D scaffold for bone tissue engineering. Acta Biomater. 2011 May;7(5):2244–55.
13. Duailibi SE, Duailibi MT, Zhang W, Asrican R, Vacanti JP, Yelick PC. Bioengineered dental tissues grown in the rat jaw. J Dent Res. 2008 Aug;87(8):745–50.
14. Manferdini C, Guarino V, Zini N, Raucci MG, Ferrari A, Grassi F, et al. Mineralization behavior with mesenchymal stromal cells in a biomimetic hyaluronic acid-based scaffold. Biomaterials. 2010 May;31(14):3986–96.
15. Perez RA, Won JE, Knowles JC, Kim HW. Naturally and synthetic smart composite biomaterials for tissue regeneration. Adv Drug Deliv Rev. 2013 Apr;65(4):471–96.
16. Shoichet MS. Polymer scaffolds for biomaterials applications. Macromolecules. 2010 Dec;43(2):581–91.
17. Costa-Pinto AR, Reis RL, Neves NM. Scaffolds based bone tissue engineering: the role of chitosan. Tissue Eng Part B Rev. 2011 Oct;17(5):331–47.
18. Rossi F, Perale G, Papa S, Forloni G, Veglianese P. Current options for drug delivery to the spinal cord. Expert Opin Drug Deliv. 2013 Mar;10(3):385–96.
19. Perale G, Rossi F, Sundstrom E, Bacchiega S, Masi M, Forloni G, Veglianese

Licensee OA Publishing London 2014. Creative Commons Attribution License (CC-BY)

FOR CITATION PURPOSES: *Pertici G, Rossi F, Casalini T, Perale G.* Composite polymer-coated mineral grafts for bone regeneration: material characterisation and model study. Annals of Oral & Maxillofacial Surgery 2014 Feb 14;2(1):4.

Competing interests: none declared. Conflict of interests: none declared.
All authors contributed to conception and design, manuscript preparation, read and approved the final manuscript.
All authors abide by the Association for Medical Ethics (AME) ethical rules of disclosure.

Annals of Oral & Maxillofacial Surgery
Open Access

P. Hydrogels in spinal cord injury repair strategies. ACS Chem Neurosci. 2011 Jul;2(7):336–45.
20. Mourino V, Cattalini JP, Roether JA, Dubey P, Roy I, Boccaccini AR. Composite polymer-bioceramic scaffolds with drug delivery capability for bone tissue engineering. Expert Opin Drug Deliv. 2013 Oct;10(10):1353–65.
21. Stevens MM. Biomaterials for bone tissue engineering. Mater Today. 2008 May; 11(5):18–25.
22. Brey DM, Chung C, Hankenson KD, Garino JP, Burdick JA. Identification of osteoconductive and biodegradable polymers from a combinatorial polymer library. J Biomed Mater Res A. 2010 May;93(2): 807–16.
23. McMahon RE, Wang L, Skoracki R, Mathur AB. Development of nanomaterials for bone repair and regeneration. J Biomed Mater Res B Appl Biomater. 2013 Feb;101(2):387–97.
24. Nelson C, Magge A, Bernard TST, Khan Y, Laurencin CT. Nanostructured composites for bone repair. J Biomater Tissue Eng. 2013 Aug;3(4):426–39.
25. Kim J, Sharma A, Runge B, Waters H, Doll B, McBride S, et al. Osteoblast growth and bone-healing response to three-dimensional poly(ε-caprolactone fumarate) scaffolds. J Tissue Eng Regen Med. 2012 May;6(5):404–13.
26. Arafat MT, Lam CX, Ekaputra AK, Wong SY, Li X, Gibson I. Biomimetic composite coating on rapid prototyped scaffolds for bone tissue engineering. Acta Biomater. 2011 Feb;7(2):809–20.
27. Perale G, Rossi F, Santoro M, Peviani M, Papa S, Llupi D, et al. Multiple drug delivery hydrogel system for spinal cord injury repair strategies. J Control Release. 2012 Apr;159(2):271–80.
28. Sturm S, Zhou S, Mai YW, Li Q. On stiffness of scaffolds for bone tissue engineering–a numerical study. J Biomech. 2010 Jun;43(9):1738–44.
29. Karande TS, Ong JL, Agrawal CM. Diffusion in musculoskeletal tissue engineering scaffolds: design issues related to porosity, permeability, architecture, and nutrient mixing. Ann Biomed Eng. 2004 Dec;32(12):1728–43.
30. Rose FR, Oreffo RO. Bone tissue engineering: hope vs hype. Biochem Biophys Res Commun. 2002 Mar;292(1):1–7.
31. Lin CY, Chang YH, Kao CY, Lu CH, Sung LY, Yen TC, et al. Augmented healing of critical-size calvarial defects by baculovirus-engineered MSCs that persistently express growth factor. Biomaterials. 2012 May;33(14):3682–92.
32. Meyer S, Floerkemeier T, Windhagen H. Histological osseointegration of Tutobone®: first results in human. Arch Orthop Trauma Surg. 2008 Jun;128(6): 539–44.
33. Kane RJ, Roeder RK. Effects of hydroxyapatite reinforcement on the architecture and mechanical properties of freeze-dried collagen scaffolds. J Mech Behav Biomed Mater. 2012 Mar;7:41–9.
34. Roveri N, Palazzo B, Iafisco M. The role of biomimetism in developing nanostructured inorganic matrices for drug delivery. Expert Opin Drug Deliv. 2008 Aug;5(8):861–77.
35. Iafisco M, Palazzo B, Marchetti M, Margiotta N, Ostuni R, Natile G, et al. Smart delivery of antitumoral platinum complexes from biomimetic hydroxyapatite nanocrystals. J Mater Chem. 2009 Sep; 19(44):8385–92.
36. Jeong SI, Lee AY, Lee YM, Shin H. Electrospun gelatin/poly(L-lactide-co-ε-caprolactone) nanofibers for mechanically functional tissue-engineering scaffolds. J Biomater Sci Polym Ed. 2008 Apr;19(3): 339–57.
37. Rossi F, Casalini T, Raffa E, Masi M, Perale G. Bioresorbable polymer coated drug eluting stent: a model study. Mol Pharmceutics. 2012 May;9(7): 1898–910.
38. Perale G, Arosio P, Moscatelli D, Barri V, Muller M, Maccagnan S, Masi M. A new model of resorbable device degradation and drug release: transient 1-dimension diffusional model. J Control Release. 2009 Jun;136(3):196–205.
39. Pertici G, Muller M, Perale G. Bioresorbable bioactive matrix for bone regeneration. Tissue Eng Part A. 2010 Aug;16(8):A–10.
40. Pertici G. Bone implant matrix and method of preparing the same. World Organization for Intellectual Property application pubblication nr. WO 2010/070416 A1, 2010.
41. Casalini T, Masi M, Perale G. Drug eluting sutures: a model for in vivo estimations. Int J Pharm. 2012 Jun;429(1–2):148–57.
42. Lao LL, Peppas NA, Boey FY, Venkatraman SS. Modeling of drug release from bulk-degrading polymers. Int J Pharm. 2011 Oct;418(1):28–41.
43. Sackett CK, Narasimhan B. Mathematical modeling of polymer erosion: consequences for drug delivery. Int J Pharm. 2011 Oct;418(1):104–14.
44. Perale G, Casalini T, Barri V, Muller M, Maccagnan S, Masi M. Lidocaine release from polycaprolactone threads. J Appl Polym Sci. 2010 Sep;117(6):3610–4.
45. Rehman I, Bonfield W. Characterization of hydroxyapatite and carbonated apatite by photo acoustic FTIR spectroscopy. J Mater Sci Mater Med. 1997 Jan;8(1):1–4.
46. Karageorgiou V, Kaplan D. Porosity of 3D biomaterial scaffolds and osteogenesis. Biomaterials. 2005 Sep;26(27):5474–91.
47. Lauzon MA, Bergeron E, Marcos B, Faucheux N. Bone repair: new developments in growth factor delivery systems and their mathematical modeling. J Control Release. 2012 Sep;162(3):503–20.
48. Tracy MA, Ward KL, Firouzabadian L, Wang Y, Dong N, Qian R, Zhang Y. Factors affecting the degradation rate of poly(lactide-co-glycolide) microspheres in vivo and in vitro. Biomaterials. 1999 Jun;20(11):1057–62.
49. Bird RB, Stewart WE, Lightfoot EN. Transport phenomena. 2nd ed. New York, NY: Wiley; 2002.

Licensee OA Publishing London 2014. Creative Commons Attribution License (CC-BY)

FOR CITATION PURPOSES: *Pertici G, Rossi F, Casalini T, Perale G.* Composite polymer-coated mineral grafts for bone regeneration: material characterisation and model study. Annals of Oral & Maxillofacial Surgery 2014 Feb 14;2(1):4.

Competing interests: none declared. Conflict of interests: none declared.
All authors contributed to conception and design, manuscript preparation, read and approved the final manuscript.
All authors abide by the Association for Medical Ethics (AME) ethical rules of disclosure.